MODELLING AND ANALYSIS OF HYDRAULIC STEP-DOWN SWITCHING CONVERTERS

Victor J. De Negri[1], Marcos P. Nostrani[1], Pengfei Wang[2], D. Nigel Johnston[2], and Andrew Plummer[2]
[1]Federal University of Santa Catarina, Department of Mechanical Engineering, LASHIP, Trindade, Florianópolis, SC, 88040-900, Brazil, e-mail: victor.de.negri@ufsc.br, marcos.nostrani@gmail.com
[2]University of Bath, Department of Mechanical Engineering, PTMC, Claverton Down, Bath, BA27AY, United Kingdom, e-mail: p.wang@live.co.uk, ensdnj@bath.ac.uk, arp23@bath.ac.uk.

Abstract

In this study, a detailed analysis of step-down converter systems, considering the load losses at the inertance tube and switched valve, is presented. The model describes the behavior of the load pressure as a function of the pulse-width modulated (PWM) duty cycle. The expressions for the load flow rate, high and low supply flow rates, and system efficiency are also discussed. A system prototype was developed on a test rig to evaluate the model accuracy. The system parameters (e.g., tube diameter and length and switching frequency) were analyzed to predict the best system configuration. The study describes how the system efficiency is influenced by these parameters. The present model and procedure allow determining the ideal parameter combination for maximum efficiency and time response of the valve.

Keywords: Digital hydraulics, Hydraulic switching converter, Hydraulic valve, PWM switched valve.

1. Introduction

Recently, the energy efficiency of hydraulic systems is a hot discussion topic by the fluid power community. Consequently, industry and academia have proposed alternatives on the scope of component and circuit designs.

It is known that the main cause of the low energy efficiency of hydraulic systems, often less than 50 %, is the extensive use of valves to throttle the flow, limit /reduce the hydraulic pressure, or reduce the flow rate on a hydraulic circuit.

In this context, there are two approaches being studied in order to achieve better efficiency systems: analogic control of pumps and motors and digital hydraulics. The first one includes variable displacement pumps and motors (Eggers et al., 2005) and fixed or variable pumps driven by variable speed electrical motors (Willkomm et al., 2014).

Research on digital hydraulic systems has intensified since the beginning of the 21st century (Scheidl et al., 2011). Basically, there are two conceptions using fundamentally on/off valves that can be integrated or a nonhydraulic power conversion component such as a pump and/or a motor.

An example of an integrated system is the digital piston pump in which the on/off valves are individually connected to each piston (Rampen, 2006, Linjama, 2011, Karvonen et al, 2014). Multichamber cylinders controlled by parallel valves switching different pressure sources (Heitzig et al., 2012; Heitzig and Theissen, 2011) and fixed displacement pumps and motors with output/input flow rates controlled by pulse-modulated valves or parallel valves (Linjama, 2011) are examples of hydraulic components with on/off valves connected to their ports.

These system configurations can be considered as digital energy conversion units. Moreover, new arrangements of valves are being studied for interconnecting conventional pumps and actuators to replace the directional proportional valves or flow control valves. The digital flow control unit combines restrictions with on/off valves (Linjama, 2011). Another alternative is the switched-reactance hydraulics that comprises a circuit composed of at least a pulse-width modulated (PWM) valve and a tube of relatively long length and small diameter.

The switched-reactance hydraulics was studied by Brown in the 1980s (Brown, 1987; and Brown et al., 1988). This type of hydraulic control is based on the cyclical acceleration and deceleration of fluid or a solid

inertance using PWM. There is a direct analogy of this hydraulic system with electrical switched power converters used extensively nowadays. The flow or pressure control of the switched-reactance hydraulics is not dissipative, thus high energy efficiency is expected. However, as shown in this study and in De Negri et al. (2014), the valve and tube load losses can reduce the efficiency considerably. Brown (1987) alerted about efficiency drop related to tube viscous friction but he did not model it. Brown (1988) and Manhartsgruber et al. (2005) presented dynamic models of switching hydraulic systems including friction. On those papers the objective was not to present a steady-state lumped parameter model as discussed in the present study.

Scheidl et al. (2008) presented an overview of switching control principles, including the buck converter (step-down transformer) investigated by Brown (1987). Brown et al. (1988), Hettrich et al. (2009) Wang et al. (2011a), and Wang et al. (2011b) presented time responses using lumped parameter modelling where the tube and/or valve load loss were included. Manhartsgruber et al. (2005) presented a frequency and time-domain model of a step-down circuit. Brown (1987), Kogler and Scheidl (2008), and Johnston (2009) showed steady-state equations for average-values of pressure and flow rates not considering load losses.

Kogler & Manhartsgruber (2009) presented an expression for the average flow rate through the tube, taking into account the tube resistance, but the dependence of the output pressure and other flow rates through the system on the tube resistance and switching frequency was not the study focus. Dynamic time responses of a linear hydraulic drive controlled by a buck converter are analyzed. Wang et al. (2011b) studied a step-down system driving a hydraulic system using a flywheel. They deduced an expression for the average load pressure as a function of the motor viscous friction and mechanical efficiency. However, they did not take into account these losses on their theoretical and experimental analyses.

In this study, a detailed modeling of a step-down transformer comprising one three-port on/off valve and an inertance tube is presented. The modeling strategy is an extension of a previous study by current authors for a step-up configuration.

The model is experimentally validated and can be used for the steady-state analysis and design of this type of device in general. Based on the equations presented, the performance related to energy efficiency is analyzed, facilitating determination of the best values for the tube diameter and length and the switching frequency.

This paper is organized as follows. In section 2, the fundamentals of the step-down converter is described. In section 3, the hydraulic step-down converter is modeled, including the resistance associated with the tube and switching orifices. Section 4 presents the experimental setup and the system parameters. In section 5, the experimental and theoretical results for different switching times are compared, confirming the model validity. Section 6 presents an analysis of the system parameters (e.g., tube diameter and length and switching frequency) and describes how the system efficiency is affected. Section 7 concludes the paper.

2. Step-Down Converter

Fig. 1 shows the fundamental circuit of a hydraulic step-down switching converter and its corresponding electrical system. A single solenoid spring return directional valve is driven by a PWM signal, modulating the time at which each flow path remains active. A hydraulic tube is connected to the valve port A, which introduces the inertance (L) and also the hydraulic resistance (R) and capacitance (C) effects. As will be discussed in the following sections, the resistance has a significant effect on the system performance; therefore, it is included in the mathematical modeling.

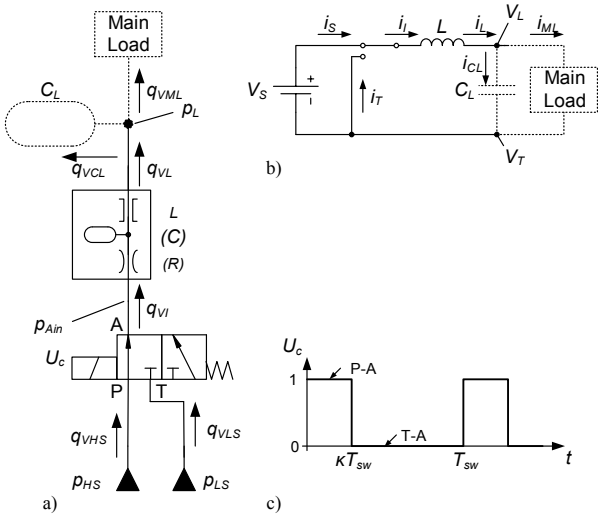

Fig. 1: Step-down converter: a) Hydraulic circuit; b) Electrical circuit; c) PWM input signal.

As can be seen in Fig. 1, when the flow path P-A is active, the internal pressure (p_{Ain}) tends to increase. Consequently, the fluid accelerates through the tube. When the valve switches to the other position, the internal chamber is connected to the port (T). However, the fluid momentum causes the fluid to continue to move through the tube, drawing the fluid from the port (T) despite the adverse (low to high) pressure gradient

between the low pressure supply port (T) and the load output. When the duty cycle (κ) is equal to 100% (P-A and T are blocked), the load pressure (p_L) is ideally equal to both p_{Ain} and the high supply pressure (p_{HS}). When $\kappa = 0\%$, the T port is connected to A, and P is blocked such that p_L and p_{Ain} are equal to the low supply pressure (p_{LS}). Ideally, the load pressure (p_L) can be modulated from the low supply pressure value to the high supply pressure value, proportional to the duty cycle.

The step-down circuit is a pressure regulator in the same manner that an electrical converter is a voltage regulator. Therefore, the average flow rate consumed by the load is a perturbation signal for the system and, as discussed in the following sections, it reduces the regulated pressure.

3. Step-Down PWM Valve Modeling

Assuming that the load capacitance (C_L) in the step-down circuit shown in Fig. 1 is sufficiently high for the load pressure (p_L) to be considered constant, the switching circuit can be analyzed separately from the main load system.

Therefore, the step-down system can be modeled on the basis of the circuit shown in Fig. 2, where Δp corresponds to the pressure drop through both the directional valve and inertance tube and q_{VI} is the inertance tube flow rate.

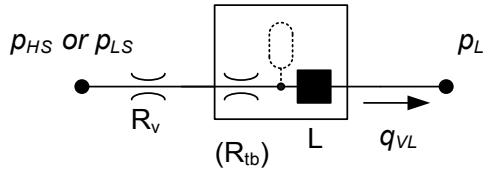

Fig. 2: Step-down fundamental hydraulic circuit with resistances.

As previously stated, in the step-down circuit, there are two different valve flow paths at the tube upstream that are switched alternately. These consequently connect the high supply (p_{HS}) or the low supply (p_{LS}) lines to the tube. Assuming that both valve flow paths have the same resistance (R_v) and the tube resistance is R_{tb}, the circuit model is given by

$$\frac{L}{R}\frac{dq_{VI}}{dt} + q_{VI} = \frac{1}{R}\Delta p\,, \tag{1}$$

where $\Delta p = p_{HS} - p_L$ for $0 \le t \le \kappa T_{sw}$,
$\Delta p = p_{LS} - p_L$ for $\kappa T_{sw} \le t \le T_{sw}$,
and $R = R_v + R_{tb}$.

Based on the approach by Millman & Taub (1965) for electric circuits, the time response of this hydraulic system for a square-wave input can be expressed by

$$q_{V1}(t) = \frac{p_{HS} - p_L}{R} + (q_{V1}(0) - \frac{p_{HS} - p_L}{R})e^{-t/\tau} \tag{2}$$
for $0 \le t \le \lambda T_{sw}$

and

$$q_{V2}(t) = \frac{p_{LS} - p_L}{R} + (q_{V2}(\kappa T_{sw}) - \frac{p_{LS} - p_L}{R})e^{-(t-\kappa T_{sw})/\tau} \tag{3}$$
for $\kappa T_{sw} \le t \le T_{sw}$,

where $\tau = L/R$.

Fig. 3a shows the graphical representation of these functions and their specific values at 0, κT_{sw}, and T_{sw} instants. As demonstrated by Millman & Taub (1965), the average output value (q_{VI}) is equal to the average input value (Δp) multiplied by the steady-state gain for an entire period. Fig. 3b presents a specific condition where the duty cycle is equal to 50%.

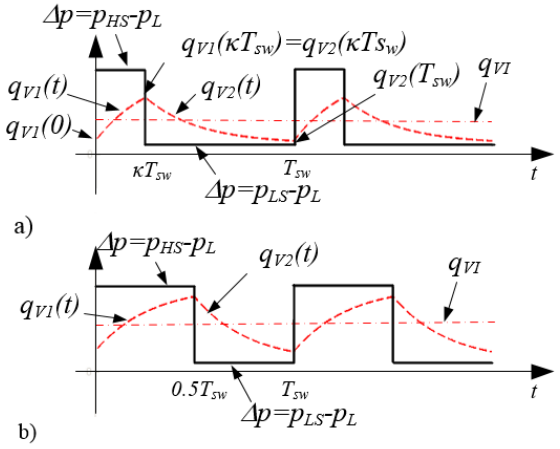

Fig. 3: Inertance tube response for a square wave (system with resistance): a) General response; b) Response for $\kappa = 0.5$.

Calculating the high pulse flow rate at $t = \kappa T_{sw}$, i.e., $(q_{V1}(\kappa T_{sw}) = q_{V2}(\kappa T_{sw}))$ and the low pulse flow rate at $= T_{sw}$, i.e., $(q_{V2}(T_{sw}) = q_{V1}(0))$, the amplitude of the flow wave can be expressed by

$$\Delta q_{VI} = \Delta q_{V1} = \Delta q_{V2} = \frac{(1 - e^{-(1-\kappa)T/\tau} - e^{-\kappa T/\tau} + e^{-T/\tau})}{(1 - e^{-T/\tau})} \cdot \frac{(p_{HS} - p_{LS})}{R}. \tag{4}$$

Following De Negri et al. (2013), for the step-up converter, the average flow rate through the inertance tube (q_{VL}), average high supply flow rate (q_{VHS}), and average low supply flow rate (q_{VLS}), respectively, can be obtained from Eqs. (2) and (3) to give

$$q_{VL} = \frac{(p_{LS} - p_L)(1-\kappa)}{R} + \frac{(p_{HS} - p_L)\kappa}{R}, \tag{5}$$

$$q_{VHS} = \frac{\tau(1-e^{-T_{sw}(1-\kappa)/\tau})(1-e^{-T_{sw}\kappa/\tau})(p_{LS}-p_{HS})}{(1-e^{-T_{sw}/\tau})RT_{SW}} + \\ + \frac{(p_{HS}-p_L)\kappa}{R}, \tag{6}$$

and

$$q_{VLS} = \frac{\tau(1-e^{-T_{sw}(1-\kappa)/\tau})(1-e^{-T_{sw}\kappa/\tau})(p_{HS}-p_{LS})}{(1-e^{-T_{sw}/\tau})RT_{SW}} + \\ + \frac{(p_{LS}-p_L)(1-\kappa)}{R}. \tag{7}$$

The load pressure can be written from Eq. (5) as a function of the high supply pressure, low supply pressure, average load flow rate, and duty cycle as

$$p_L = (p_{HS}-p_{LS})\kappa + p_{LS} - q_{VL}R. \tag{8}$$

Eq. (8) shows that the load pressure in a step-down converter does not depend on the switching period, and has a linear behavior with respect to the duty cycle. However, the flow rate required by the system causes a load loss in the tube and switching valve, which reduces the regulated pressure. Eq. (8), ignoring the last term on the right-hand side, corresponds to the ideal step-down converter (Brown, 1987; Johnston, 2009; Kogler and Scheidl, 2008).
The energy efficiency, expressed by

$$\eta = \frac{p_L q_{VL}}{p_{HS} q_{VHS} + p_{LS} q_{VLS}}, \tag{9}$$

increases as T_{sw} increases. This dependence occurs because the rate that the q_{VHS} decreases, is higher than the q_{VLS} increases as T_{sw} increases.

4. Experimental System Setup

A hydraulic circuit (Fig. 4) was implemented for the experimental study. The circuit comprises four turbine flow meters (S1, S6, S8, and S9), four strain gauge pressure transducers (S3, S4, S5, and S7), and a thermocouple (S2). The role of the directional valve shown in Fig. **1**a is performed by a directional proportional valve, V1, (Parker D1FPE50MA9NB01) whose parameters are presented in Table 1. The equivalent resistance was calculated from the experimental points, as shown in De Negri et al. (2013).

Table 1: Parameters of the proportional valve

Nominal flow rate (q_{Vn})	0.67 L/s (40L/min)@ $\Delta p_p = 3.5$ MPa [2]
Equivalent resistance (R_e)	3.88x10^9 Pa.s/m^3 @ $U_c = \pm U_{cn}$ [1]
Settling time (t_s)	3.5 ms @ $U_c = 0 \rightarrow 100\%$ [2] 6.25 ms @ U_c = -100 $\rightarrow$ +100% [1]
Natural frequency (ω_n)	120Hz@90°($U_c = \pm 90\%$) [2]

[1]Experimental data; [2]Catalogue data

The inertance tube (T1) has internal diameter (d_t) of 7.1 mm and length (l_t) of 1.7 m. The hydraulic fluid has density (ρ) 870 kg/m^3 and is assumed to have an effective bulk modulus (β_e) of 1.6x10^9 Pa. Using the Eq. (10) shown below, the tube inertance (L_t) is 3.75x10^7 kg/m^4. The hydraulic measured resistance (R_t) is 1.67x10^9 Pa.s/m^3. The equivalent resistance (R) of the valve and tube is 5.55x10^9 Pa.s/m^3.

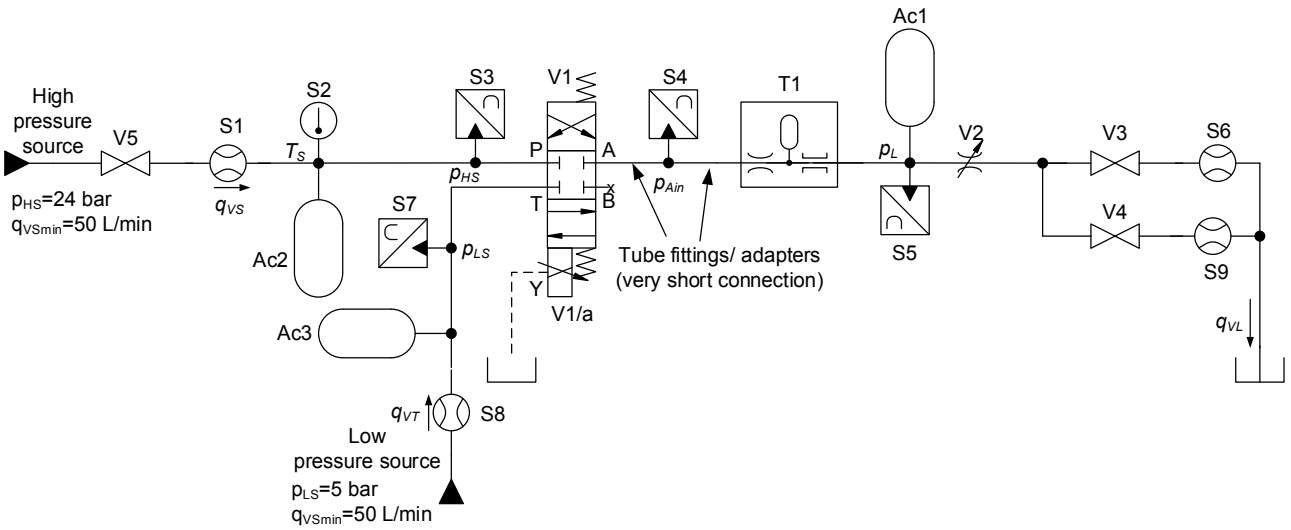

Fig. 4: Hydraulic circuit diagram.

5. Theoretical and Experimental Results

5.1. Introduction

The equations presented in Section 3 describe the steady-state behavior of a step-down PWM valve, i.e., assuming that the inputs duty cycle and average load flow rate are constant as well as the switching frequency and high and low supply pressures. The resulting responses correspond to average values in a time period.

To validate this model, experiments were conducted using the setup described in Section 4. Switching periods of 125 ms ($f_{sw} = 8$ Hz), ($f_{sw} = 16$ Hz), and 25 ms ($f_{sw} = 40$ Hz), were employed, taking into account the valve settling time shown in Table 1. For the first two periods, the spool achieved total displacements on the boundary duty cycles of 10% and 90%. As shown below, for 25 ms, the valve responded for duty cycles between 30% and 70%.

The experiments were conducted for different duty cycles while keeping the average load flow rate constant, which was adjusted by valve V2 (Fig. 4). The average high supply pressure (p_{HS}) was adjusted to 2.4 MPa, and the values of the average low supply pressure (p_{LS}) during the tests are shown in Table 2.

Table 2: Average low supply pressures.

Load flow rate	Average low supply pressure		
	For $T_{sw} = 125$ ms	For $T_{sw} = 62.5$ ms	For $T_{sw} = 25$ ms
0 L/s	0.22 MPa	0.25 MPa	0.23 MPa
0.1 L/s	0.20 MPa	0.21 MPa	0.22 MPa
0.2 L/s	0.17 MPa	0.19 MPa	0.20 MPa
0.3 L/s	0.15 MPa	0.19 MPa	0.16 MPa

5.2. Switching Period of 125 ms

Fig. 5 presents the load pressure controlled by the step-down converter as a function of the duty cycle and load flow rate. The switching frequency (f_{sw}) is 8 Hz ($T_{sw} = 125$ ms). As one can see, the tube and valve load losses have a large influence on the system performance, and thus, the regulated pressure is reduced as the load flow rate increases. In this figure, and in the following ones, the lines correspond to the theoretical results according to the equations presented above, whereas the points correspond to the experimental results.

The experimental values in Fig. 5 demonstrate that the load pressure has a linear dependence on the duty cycle and its magnitude depends on the load flow rate (q_{VL}), as denoted by Eq. (8). Since a linear, rather than a square root, function of the flow rate with the valve pressure drop is assumed, the theoretical results differ from experimental ones as the flow rate through the valve increases. The valve characteristic curves are shown in De Negri et al. (2013).

Furthermore, negative pressures can be determined numerically, but they do not occur in practice because of the air solubility and/or fluid vaporization at such conditions. Therefore, the achieved minimal value of the duty cycle that results in a load pressure equal to the low supply pressure increases as the flow rate to the load system increases.

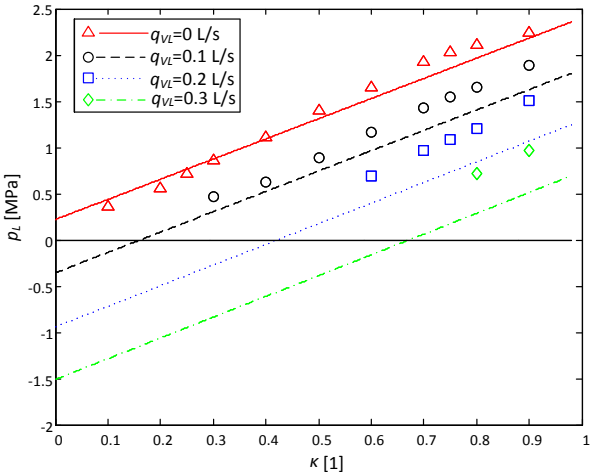

Fig. 5: Load pressure versus duty cycle for 8 Hz.

Fig. 6 and Fig. 7 present the average high and low supply flow rates, respectively, where the experimental points confirm the model prediction.

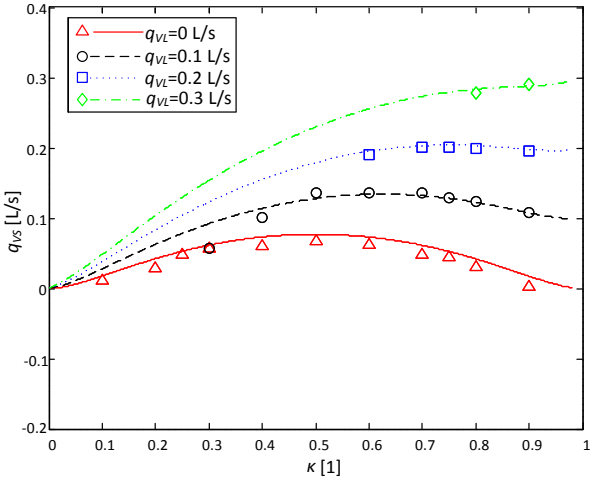

Fig. 6: High supply flow rate versus duty cycle for 8 Hz.

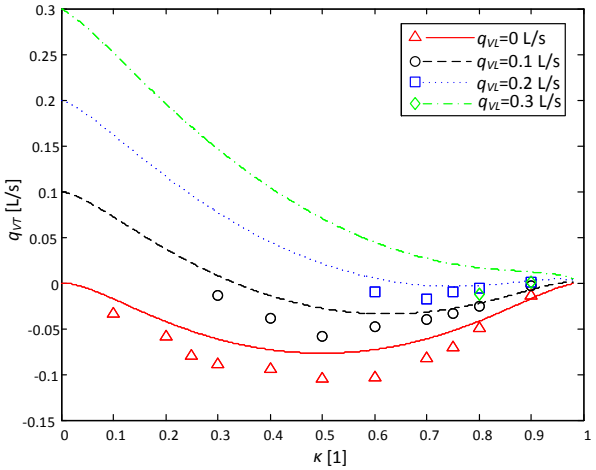

Fig. 7: Low supply flow rate versus duty cycle for 8 Hz.

5.3. Switching Periods of 62.5 ms and 25 ms

Theoretical and experimental results under the same conditions as those described in the Section 5.1 were also obtained using the switching frequencies (f_{sw}) of 16 Hz (T_{sw} = 62.5 ms) and 40 Hz (T_{sw} = 25 ms).

Fig. 8 presents the load pressure for 16 Hz. At 16 Hz, the pulse time at 10% and 90% is 6.25 ms, which is equal to the valve settling time. As the valve dynamic response is not considered in the modeling, one can conclude that the valve opening transient does not introduce substantial load loss as the valve achieves its full opening.

The good proximity of the experimental points in relation to the theoretical curves corroborates the model adequacy.

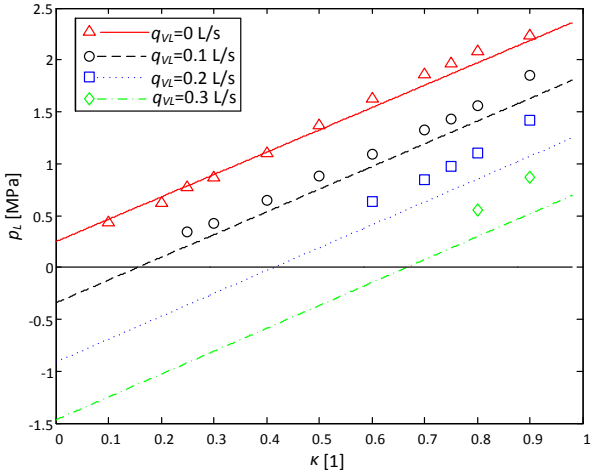

Fig. 8: Load pressure versus duty cycle for 16 Hz.

Experimental and numerical results using a switching frequency (f_{sw}) of 40 Hz (T_{sw} = 25 ms) are shown in Fig. 9 and Fig. 11. As can be observed, the general shape of the curves is as predicted by the model, but the effective behavior is in consistent, as is the case with lower switching frequencies.

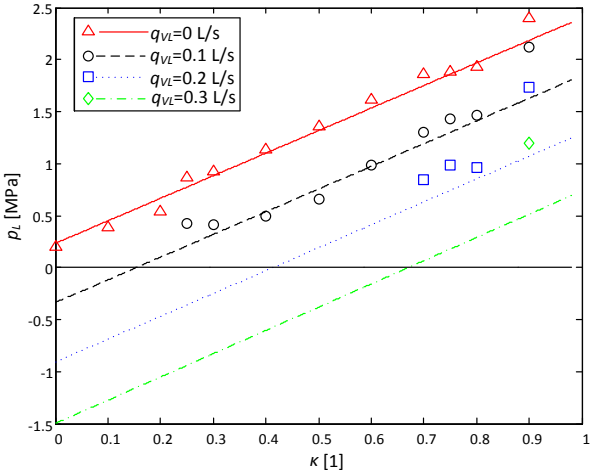

Fig. 9: Load pressure versus duty cycle for 40 Hz.

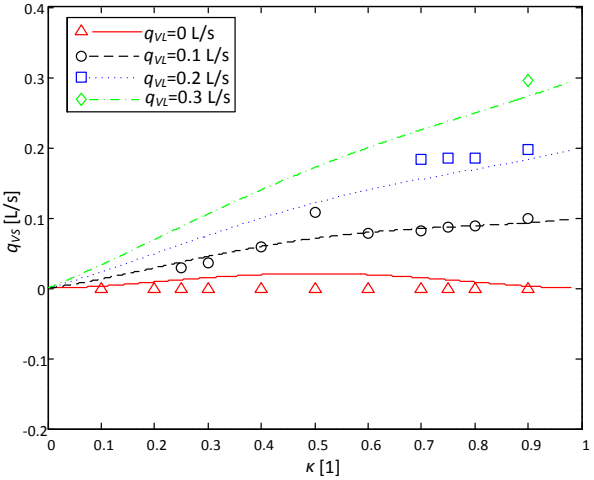

Fig. 10: High supply flow rate versus duty cycle for 40 Hz.

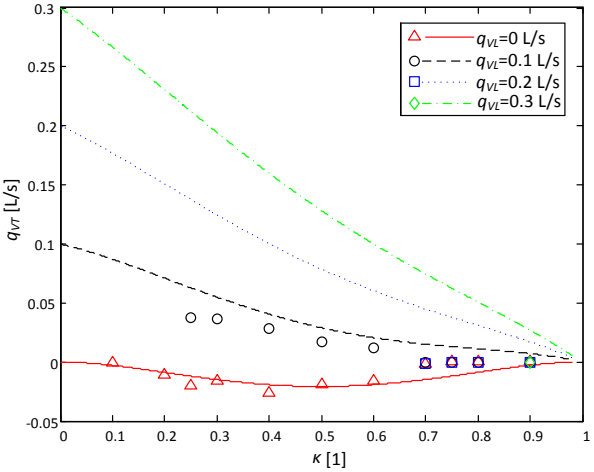

Fig. 11: Low supply flow rate versus duty cycle for 40 Hz

For 40 Hz, the valve does not respond fast enough, particularly, for boundary duty cycles. For example,

Fig. 12a shows the dynamic valve spool position for a duty cycle of 40% when the valve achieves the final position at each pulse. However, for a duty cycle of 90% (Fig. 12b), the valve is unable to fully connect ports A and T. Consequently, the load pressure and high supply flow rate are higher, whereas the low supply flow rate is lower than the theoretical values (Fig. 9–Fig. 11).

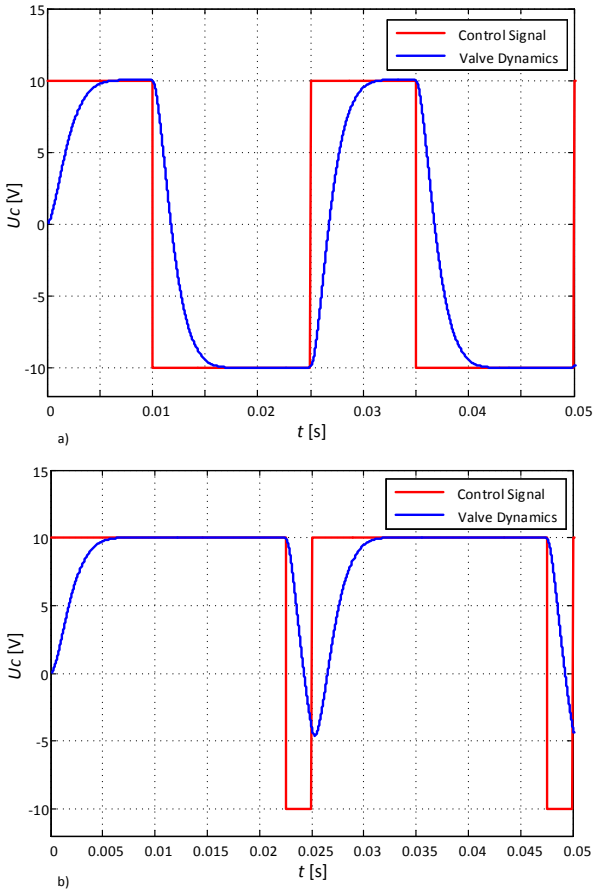

Fig. 12: Valve response a) κ=0.4, b) κ= 0.9.

Generally, for lower duty cycles, when the valve does not achieve the full opening of P to A and a full closing to port T, the regulated pressure and high supply flow rate tend to be lower than that expected. Conversely, for higher duty cycles, the regulated pressure is higher and the low supply flow rate is lower than that expected.

6. Parameter Optimization

6.1. Diameter and Length

As discussed in the previous section, the theoretical estimates are valid, as the valve can achieve full opening and closing during a time period.

The step-down converter efficiency, expressed by Eq. (9), changes with the duty cycle. It also depends on the component parameters, i.e., the tube inertance and resistance, valve resistance, and switching period.

The tube inertance, determined by

$$L = \frac{4\rho l_t}{\pi d_t^2}, \tag{10}$$

and the tube resistance for a laminar flow, calculated by

$$R = \frac{128\rho l_t \mu}{\pi d_t^4}, \tag{11}$$

depend on the tube diameter and length. Therefore, the system performance can be evaluated according to the two basic parameters.

Based on practical principles, the following analysis considers a tube diameter between 5 to 20 mm. The minimal tube length is calculated by $l_t = 138 d_t$ for laminar flow (Fox et al., 2011), and the maximum length is assumed as 20 m.

The simulations were performed with high supply pressure (p_{HS}) of 12 MPa, low supply pressure (p_{LS}) of 0.3 MPa, and load flow rate (q_{VL}) of $2x10^{-4}$ m^3/s. The fluid properties are the same as those presented in Section 4.

Considering a switching frequency of 40 Hz (T_{sw} = 25 ms) and duty cycle (κ) adjusted to 0.5, Fig. 13 shows how the different combinations of tube diameter and length affect the step-down efficiency.

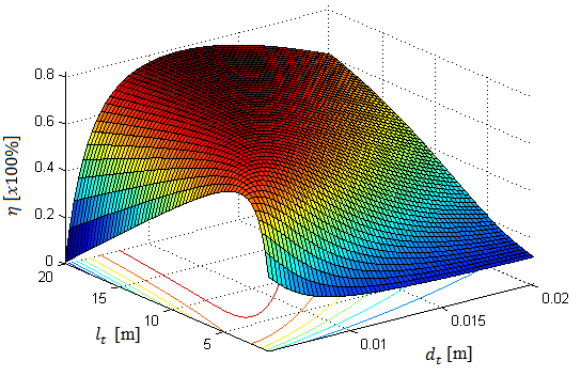

Fig. 13: Step-down efficiency versus tube diameter and length for κ=0.5.

The results shown in Fig. 13 demonstrate that the efficiency increases with increasing tube length for tube diameters higher than 10 mm. For lower diameter values, an optimum tube length (20 m) provides maximum efficiency. Fig. 14 shows the efficiency behavior for tube diameters varying from 6 mm to 15 mm.

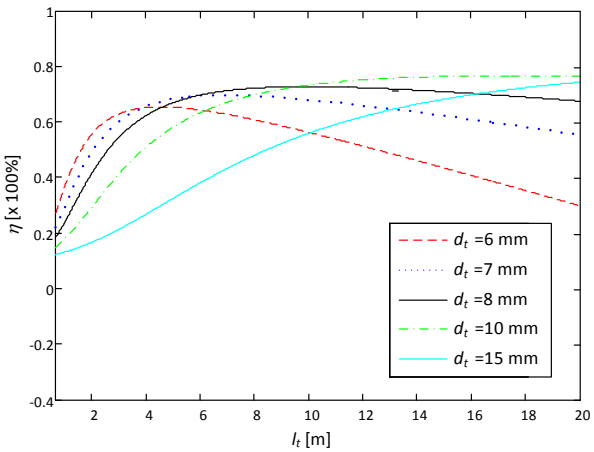

Fig. 14: Step-down efficiency for different tube diameters.

The higher efficiency values are associated with higher tube lengths, but the variation shows no significant difference in efficiency for lengths and diameters greater than 20 m and 10 mm, respectively.

Using a 20 m long tube is impracticable for real applications. Therefore, some strategy must be applied to achieve an ideal tube diameter and length without great efficiency loss. In this study, the largest efficiency value that could be achieved in a tube of length 20 m was determined, and this value was further reduced by 10%. Table 3 shows the results.

Table 3: Optimum values of tube length and diameter.

Efficiency (×100%)	Length (m)	Diameter (m)
0.77	20.0	0.0110
0.69	6.1	0.0071

6.2. Switching Time

As shown in sections 3 and 5, the switching frequency has a significant influence on the average high and low supply flow rates. Consequently, the switching frequency directly influences the step-down efficiency (Eq. (9)). Fig. 15 shows how the efficiency varies with different values of switching frequencies. The tube diameter and length are 7 mm and 6 m, respectively, based on the results presented above.

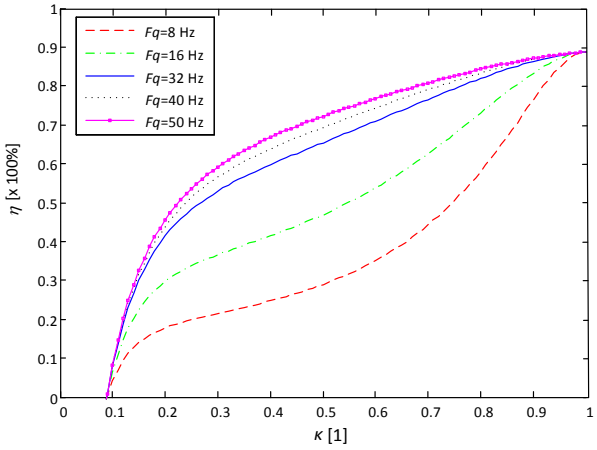

Fig. 15: Efficiency versus duty cycle for different switching frequencies.

As shown in Fig. 15, when the switching frequency is increased, the efficiency increases for intermediate values of the duty cycle. Frequencies of 32 Hz (T_{sw} = 31.25 ms) and 40 Hz (T_{sw} = 25 ms) result in very similar efficiencies. Fig. 16 shows the efficiency for switching frequencies from 8 Hz (T_{sw} = 125 ms) to 150 Hz (T_{sw} = 6.6 ms) which shows that the subsequent frequency increase from 50 Hz does not contribute significantly to the system performance.

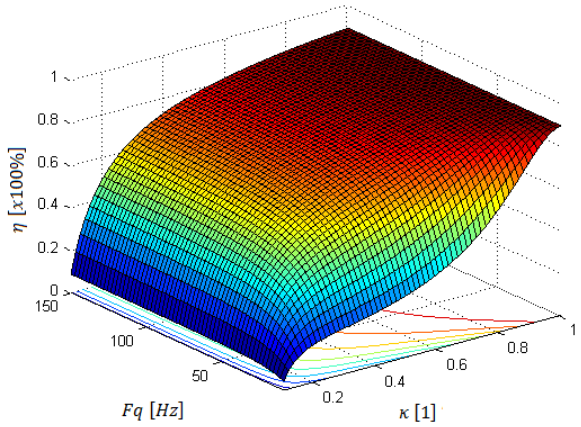

Fig. 16: Efficiency for switching frequencies from 8 Hz to 150 Hz.

Fig. 15 and Fig. 16 show that the efficiency is not significantly improved using switching valves with extremely high time response. For example, for 50 Hz, valves with settling times of 2 ms are qualified for operation with duty cycles between 10% and 90%. Valves with such dynamic performance are being developed by research institutes (Winkler et al., 2008, Uusitalo et al., 2010, and Winkler et al., 2010). Commercial valves up to 10 ms are reported by (Linjama and Vilenius, 2008, Murrenhoff, 2003).

7. Conclusions

A detailed model of the step-down PWM valve, which is of interest for the analysis and design of new systems based on the switched inertance principle is presented. Using the model that includes linear resistance, theoretical and experimental results show that it is possible to predict the average value of the controlled pressure and flow rates at the step-down converter ports.

Therefore, despite the flow-pressure nonlinearity and the limited time response of the switching valve as well as the pressure wave propagation in the inertance tube, the presented linear model describes the global behavior of step-down switching converters.

The dynamic behavior of switching converters is complex. Several phenomena occur such as fluid compressibility in the internal chambers and wave propagation through the tube. Determining the system performance and the effectiveness of the design on the basis of this information alone is difficult. In this context, the proposed model can be used for the preliminary design of switching converters, and a time or frequency analysis can be performed for system optimization.

According to the equations presented, in the step-down converter, the average high and low supply flow rates depend on the PWM signal period, resistance, inertance and the average load flow rate, but the load pressure does not depend on the switching period. A study of the parameters of the inertance tube (diameter and length) and switching period was conducted; thus, a procedure to predict the best combination for the optimum efficiency in each case could be found. This procedure involves determining a higher efficiency value for a tube length of 20 m and reducing this value by 10%. Consequently, the tube length is reduced significantly without incurring a high efficiency loss.

The switching period directly influences the system efficiency; however, for high values, the variation in efficiency is insignificant. The valve dynamics must be sufficiently high to operate with duty cycles between 10% and 90%. Therefore, using this model and procedure, it is possible to determine the ideal parameter combination for maximum efficiency and time response of the valve.

References

Brown, F. T. 1987. Switched reactance hydraulics: a new way to control fluid power. Proc. National Conference on Fluid Power. Chicago, USA, pp. 25-34.

Brown, F.T. Tentarelli, S. C., Ramachandran, S. A. 1988. A hydraulic rotary switched-inertance servo-transformer, Transactions of ASME: Journal of Dynamic Systems, Measurement, and Control. Vol. 110, pp.144-150.

Eggers, B., Rahmfeld, R., Ivantysynova., M. 2005. An energetic comparison between valveless and valve controlled active vibration damping for off-road vehicles. Proceedings of the 6th JFPS International Symposium on Fluid Power. TSUKUBA.

Fox, R. W., McDonald, A. T., and Pritchard, P. J. 2011. Introduction to Fluid Mechanics, 8th ed.

Hettrich, H., Bauer, F., Fuchshumer, F. 2009. Speed controlled, energy efficient fan drive within a constant pressure system. Proceedings of the Second Workshop on Digital Fluid Power. Linz, Austria, pp. 62-71.

Johnston, D. N. 2009. A switched inertance device for efficient control of pressure and flow. Proceedings of the ASME 2009 Dynamic Systems and Control Conference - DSCC2009. Hollywood, USA.

Karvonen. M., Heillia. M. Huova, M., Linjama, M. 2014. Analysis by simulation of diferente control algorithms od a digital hydraulic two-actuator system. International Journal of Fluid Power. Vol. 15. N. 1. Pp. 33-44.

Kogler, H., Scheidl, R. 2008. Two basic concepts of hydraulic switching converters. Proceedings of the First Workshop on Digital Fluid Power. Tampere, Finland, pp. 113-128.

Kogler, H., Manhartsgruber, B. 2009. Simulation tools and control design for fast switching hydraulic sustems. Proceedings of the Second Workshop on Digital Fluid Power. Linz, Austria, pp. 85-93.

Linjama, M. 2011.Digital fluid power-state of the art. *The Twelfth Scandinavian International Conference on Fluid Power*, Tampere, Finland.

Linjama, M., Vilenius, M. 2008. Digital Hydraulics – Towards Perfect Valve Technology. Technology. Digitalna Hidravlika, Ventil 14 / 2008/ 2. pp. 138-148.

Manhartsgruber, B., Mikota, G., Scheidl, R. 2005. Modelling of a switching control hydraulic system. Mathematical and Computer Modelling of Dynamical Systems, Vol. 11, N. 3, pp. 329-344.

Millmann, J., Taub, H. 1965. Pulse, digital, and switching waveforms. McGraw-Hill, New York.

Murrenhoff, H. 2003. Trends in valve development. O+P – Ölhydraulik und Pneumatik. Vol. 46, N. 4.

Rampen, W. 2006. Gearless Transmissions for Large Wind Turbines–The history and Future of Hydraulic Drives. Dewek Bremen.

Scheidl, R., Manhartsgruber, B., Winkler, B. 2008. Hydraulic Switching control – Principles and state of the art. Proceedings of the First Workshop on Digital Fluid Power. Tampere, Finland, pp. 31-49.

Scheidl, R., Linjama, M., Schmidt, S. 2011. Is the Future Of Fluid Power Digital? Proceedings of the Institution of Mechanical Engineers. Part I: Journal of Systems and Control Engineering, v. 226, n. 6, p pp. 721-723, 2012. ISSN 09596518.

Uusitalo,J.-P., Ahola, V., Soederlund, L., Linjama, M., Juhola, M., Kettunen, L. 2009. Novel bistable hammer valve for digital hydraulics. International Journal of Fluid Power. N. 3, pp. 35-44.

Wang, P., Sylwester, K., Johnston, N., Plummer, A., Hillis, A. 2011a. The influence of wave effects on digital switching valve performance. Proceedings of the Fourth Workshop on Digital Fluid Power. Linz, Austria, pp. 10-25.

Wang, F. Gu, L., Chen, Y. 2011b. A continuously variable hydraulic pressure converter based on high-speed on–off valves. Mechatronics. N. 21. pp. 1298-1308.

Willkomm, J., Wanler, M., Weber., J. 2014. Process-adapted control to maximize dynamics of displacement-variable pumps. Symposium on Fluid Power & Motion Control. Bath, United Kingdom. pp. 10-12.

Winkler, B., Plöckinger, A., Scheidl, R. 2008. Components for digital and switching hydraulics. Proceedings of the First Workshop on Digital Fluid Power. Tampere, Finland. pp. 53-76.

Winkler, B., Plöckinger, A., Scheidl, R. 2010. A novel piloted fast switching multi popet valve. International Journal of Fluid Power. N. 3, pp. 7-14.